

See discussions, stats, and author profiles for this publication at: <https://www.researchgate.net/publication/231400218>

Theoretical study of anion–molecule interactions: hydride + hydrogen fluoride .fwdarw. hydrogen + fluoride

ARTICLE *in* THE JOURNAL OF PHYSICAL CHEMISTRY · FEBRUARY 1991

Impact Factor: 2.78 · DOI: 10.1021/j100156a011

CITATIONS

12

READS

12

4 AUTHORS, INCLUDING:



Jeffrey Allen Nichols

Oak Ridge National Laboratory

73 PUBLICATIONS 2,427 CITATIONS

SEE PROFILE

Theoretical Study of Anion-Molecule Interactions: $\text{H}^- + \text{HF} \rightarrow \text{H}_2 + \text{F}^-$

Jeffrey A. Nichols,[†] Rick A. Kendall,[‡] Samuel J. Cole, and Jack Simons*

Department of Chemistry, University of Utah, Salt Lake City, Utah 84112 (Received: July 2, 1990)

We present results of ab initio multiconfigurational SCF (MCSCF), fourth-order perturbation theory MBPT(4), and coupled-cluster CCSD(T) electronic structure simulations on the ground-state $\text{H}^- + \text{HF} \rightarrow \text{H}^-\text{HF} \rightarrow \text{H}_2\text{F}^- \rightarrow \text{H}_2 + \text{F}^-$ potential energy hypersurface. Structures, energetics, and local harmonic vibrational frequencies are included in this study. The H_2F^- ion-molecule complex is found to be linear; the anticipated H^-HF complex is found to be an unstable inflection point on the surface, (i.e., no bound minimum corresponding to H^- bound to an HF moiety exists). Vertical detachment at the F^-H_2 complex geometry to produce neutrals in $^2\Sigma$ and $^2\Pi$ states is also examined.

I. Introduction

Advances and greatly expanded interest in anion spectroscopy¹⁻²² have prompted us to examine the structures and stabilities of several anion-molecule complexes (e.g., H^-H_2 , $\text{H}^-(\text{H}_2)_2$, $\text{H}^-(\text{H}_2\text{O})$, $\text{H}^-(\text{H}_2\text{O})_2$, H^-NH_3 , H^-CH_4 , and H^-Ne).²³⁻²⁵ In this paper we present the results of our investigation of the ground state of the $(\text{H}_2\text{F})^-$ complex. Included in this study is an examination of the reaction path connecting $\text{H}^- + \text{HF}$, through the anticipated H^-HF and H_2F^- complexes to the $\text{H}_2 + \text{F}^-$ species. Energetics, structures, and (harmonic) vibrational frequencies are examined. This particular anion is of special relevance to the experiments of the Neumark group^{21,22} and forms the underlying anion species for the much studied $\text{F} + \text{H}_2$ reaction.²⁶

The theoretical study of such anion-molecule complexes is complicated by several factors: (1) the complexation energies are small (only a few kcal/mol), so reasonably high precision calculations are essential; (2) treatment of the highly polarizable anion requires special basis sets; (3) interactions among several permanent (e.g., dipole, quadrupole) and induced moments contribute to the net interaction energy and to the angular dependence of this energy which, in turn, determine the equilibrium "shapes" of the complexes; (4) tracing reaction paths through transition states requires the use of an efficient potential energy surface walking algorithm and may necessitate the inclusion of more than one dominant electronic configuration; (5) the electron binding energy of the anion may vary considerably throughout the reaction path (as it does for $\text{H}^- + \text{HF} \rightarrow \text{H}_2 + \text{F}^-$), and the anion may even become unstable with respect to electron autodetachment at points along the path. As discussed later in this paper, our Utah MESS-KIT software²⁷ allows us to address each of these features. In section II we give the details of our calculations and then present and discuss our findings in section III.

II. Computational Details

Atomic Basis Set. The basis set for the H atoms uses the Dunning augmented correlation consistent (cc) polarized valence triple- ζ (p-VTZ) [6s3p2d|4s3p2d] basis.²⁸ The basis set²⁹ for the F atom is taken from the Dunning [11s6p3d|5s4p3d] augmented cc p-VTZ basis set. The resulting basis for the $(\text{H}_2\text{F})^-$ complex has a total of 85 contracted Gaussian functions. For the $(\text{H}_2\text{F})^-$ complex, we found basis set superposition errors to amount to no more than 1 kcal/mol for all of the methods used in this paper.

Treatment of Electronic Correlation. It is widely known that the electron pair in H^- cannot be even qualitatively described by a single $1s^2$ configuration; H^- is unstable relative to $\text{H} + e^-$ at this level of treatment. The electron pair in H^- undergoes correlated motion which necessitates at least two ($1s^2$ and $2s^2$) configurations for a qualitatively accurate description. Furthermore, to homolytically break the $\text{H}-\text{F}$ bond one cannot use only the single $1\sigma^2 2\sigma^1 1\pi^4 3\sigma^2$ configuration; a singlet-coupled configuration of the form $1\sigma^2 2\sigma^1 1\pi^4 3\sigma^2 4\sigma^1$ is also needed. Sim-

ilarly, one cannot homolytically break the $\text{H}-\text{H}$ bond using only one ($1\sigma_g^2$) configuration; the $1\sigma_u^2$ configuration is also needed. Moreover, it is well-known that achieving a balanced treatment of the electron correlation in F^- and F is extremely difficult; doing

- (1) Mead, R. D.; Stevens, A. E.; Lineberger, W. C. *Gas Phase Ion Chem.* **1984**, 3, 213.
- (2) Haberland, H.; Schindler, H.-G.; Worsnop, D. R. *Ber. Bunsen-Ges. Phys. Chem.* **1984**, 88, 270.
- (3) Coe, J. V.; Snodgrass, J. T.; Freidhoff, C. B.; McHugh, K. M.; Bowen, K. H. *J. Chem. Phys.* **1985**, 83, 3169.
- (4) Gudeman, C. G.; Saykally, R. J. *Annu. Rev. Phys. Chem.* **1984**, 35, 387.
- (5) Corderman, P. R.; Lineberger, W. C. *Annu. Rev. Phys. Chem.* **1979**, 30, 347.
- (6) Herzberg, G.; Lagerquist, A. *Can. J. Phys.* **1968**, 46, 2363.
- (7) See ref 5.
- (8) Zheng, L. S.; Karner, C. M.; Brucut, P. J.; Yang, S. H.; Pettiette, C. L.; Craycroft, M. J.; Smalley, R. G. *J. Chem. Phys.* **1986**, 85, 1681.
- (9) Coe, J. V.; Snodgrass, J. T.; Freidhoff, C. B.; McHugh, K. M.; Bowen, K. H. *J. Chem. Phys.* **1985**, 83, 3169.
- (10) Lykke, K. R.; Mead, R. D.; Lineberger, W. C.; Marks, J.; Brauman, J. I. *J. Chem. Phys.* **1984**, 81, 4883.
- (11) Neumark, D. M.; Andersen, T.; Lineberger, W. C. *J. Chem. Phys.* **1985**, 83, 4364.
- (12) Lykke, K. R.; Neumark, D. M.; Andersen, T.; Trapa, V.; Lineberger, W. C. *Springer Ser. Opt. Sci.* **1985**, 49, 130.
- (13) Al-Za'al, M.; Miller, H. C.; Farley, J. W. *Phys. Rev.* **1987**, A35, 1009.
- (14) Owrutsky, J. C.; Rosenbaum, N. H.; Tack, L. M.; Saykally, R. J. *J. Chem. Phys.* **1986**, 84, 5308.
- (15) Tack, L. M.; Rosenbaum, N. H.; Owrutsky, J. C.; Saykally, R. J. *J. Chem. Phys.* **1985**, 83, 4364.
- (16) Polak, M.; Gruebel, M.; Saykally, R. J. *J. Chem. Phys.* **1987**, 87, 3352.
- (17) Carlsten, J. L.; Peterson, J. R.; Lineberger, W. C. *Chem. Phys. Lett.* **1976**, 37, 5.
- (18) Novick, S. E.; Jones, P. L.; Mulloney, T. J.; Lineberger, W. C. *J. Chem. Phys.* **1979**, 42, 305.
- (19) Miller, T. M.; Leopold, D. G.; Murray, K. K.; Lineberger, W. C. *J. Chem. Phys.* **1986**, 85, 2368.
- (20) Coe, J. V.; Snodgrass, J. T.; Freidhoff, C. B.; McHugh, K. M.; Bowen, K. H. *J. Chem. Phys.* **1985**, 83, 3169.
- (21) Weaver, A.; Metz, R. B.; Bradforth, S. E.; Neumark, D. M. *J. Phys. Chem.* **1988**, 92, 5558.
- (22) Metz, R. B.; Kitsopoulos, T.; Weaver, A.; Neumark, D. M. *J. Chem. Phys.* **1988**, 88, 1463.
- (23) Gutowski, M.; Taylor, H.; Hernandez, R.; Simons, J. *J. Phys. Chem.* **1988**, 92, 6179.
- (24) Chalasinski, G.; Kendall, R. A.; Simons, J. *J. Chem. Phys.* **1987**, 87, 2965. Kendall, R. A.; Simons, J.; Gutowski, M.; Chalasinski, G. *J. Phys. Chem.* **1989**, 93, 621.
- (25) Chalasinski, G.; Kendall, R. A.; Simons, J. *J. Phys. Chem.* **1987**, 91, 6151.
- (26) Neumark, D. M.; Wodtke, A. M.; Robinson, G. N.; Hayden, C.; Lee, Y. T. *Phys. Rev. Lett.* **1989**, 53, 226.
- (27) The Utah MESS-KIT is a suite of highly modular codes that was programmed in-house to give a variety of electronic structure functionalities by J. A. Nichols, M. R. Hoffmann, R. A. Kendall, H. L. Taylor, D. W. O'Neal, E. Earl, R. Hernandez, M. Gutowski, J. Boatz, K. Bak, J. Anchell, X. Wang, M. Feyereisen, and J. Simons.
- (28) Dunning, Jr., T. H. *J. Chem. Phys.*, in press.
- (29) The basis for F given in ref 6 contains a single f-type orbital which we removed to form our basis.

[†] Present address: IBM Corporation, Utah Supercomputer Institute, Salt Lake City, UT.

[‡] Present address: Pacific Northwest Labs, Richland, WA.

TABLE I: Energies, Geometries, and Vibrational Frequencies for the Reaction $\text{H}_2 + \text{F}^- \rightarrow \text{HF} + \text{H}^-$

species	calculation type	energy, hartrees	geometry, ^d Å	freq, cm ⁻¹
$\text{H}^- + \text{HF}$	MCSCF	-100.673 581	$r_{\text{HF}} = 0.922$	4284
	MBPT(4)	-100.852 411		
	CCSD(T)	-100.852 148		
	CCSD(T)	-100.852 159	$r_{\text{HF}} = 0.919$	4087
	(0.0; ^a 6.1 ^b)			
H^-HF	MCSCF	-100.727 571	$r_{\text{HF}} = 1.068$, ^c $r_{\text{HH}} = 1.193$	351i, 1270, 1597
	MBPT(4)	-100.900 400		
	CCSD(T)	-100.897 824		
	(-28.7; -22.8)			
HHF^-	MCSCF	-100.741 753	$r_{\text{HF}} = 1.999$, $r_{\text{HH}} = 0.758$	292, 773, 4143
	MBPT(4)	-100.910 225		
	CCSD(T)	-100.904 416		
	CCSD(T)	-100.905 480	$r_{\text{HF}} = 1.690$, $r_{\text{HH}} = 0.770$	
	(-33.5; -25.2)			
$\text{H}_2 + \text{F}^-$	MCSCF	-100.710 779	$r_{\text{HH}} = 0.755$	4224
	MBPT(4)	-100.900 279		
	CCSD(T)	-100.894 312		
	CCSD(T)	-100.894 408	$r_{\text{HH}} = 0.730$	4378
	(-26.5; -20.5)			

^a Relative energy, based on total electronic energy only (in kcal/mol). ^b With zero-point energies added. ^c At this geometry, the gradient norm was 0.35×10^{-3} hartrees per bohr, but the Hessian matrix had one negative eigenvalue. ^d The HHF angle is 180° , corresponding to a linear geometry for all species studied.

so requires flexible basis sets and configuration interaction beyond the singly and doubly excited level.

On the basis of these observations and drawing from our experience on other anion-molecule complexes, we knew that a multiconfiguration-based wave function would be needed to achieve even a qualitatively correct treatment of this species. We therefore included in our multiconfiguration wave function all $^1\Sigma$ (or $^1A'$ for nonlinear geometries) configurations which can be formed by distributing ten valence electrons among five valence orbitals of σ character (a' in nonlinear geometry) and two pairs of degenerate π orbitals. The F atom $1s^2$ core orbital was kept doubly occupied in all configurations, although its LCAO-MO coefficients were fully optimized in the MCSCF wave function optimization. This choice of nine valence orbitals for ten valence electrons gave rise to 1436 configuration state functions. The complete active space (CAS) configuration space is known to yield size-extensive interaction energies, which is absolutely necessary when computing the weak interactions on the $(\text{H}_2\text{F})^-$ surface.

The five valence σ orbitals represent (1) the $1s$ and $2s$ orbitals of H^- , the HF bonding σ and antibonding σ^* orbitals, and the HF nonbonding σ orbital, at the $\text{H}^- + \text{HF}$ geometry, or (2) the H bonding σ and antibonding σ^* orbitals and the F^- $2s$ and $2p_\sigma$ orbitals, as well as another σ orbital (to correlate the $2p_\sigma$), at the $\text{H}_2 + \text{F}^-$ geometry. The four π orbitals represent the occupied $2p_\pi$ orbitals of HF or of F^- plus a pair of p_π orbitals on the F center to correlate the occupied $2p_\pi$ orbitals.

Analytical Energy Derivatives and Potential Energy Surface Walking. Searching for the minima (e.g., the sought after H-HF and H_2F^- complexes) and the possible transition state on the three-dimensional potential energy surface of the $(\text{H}_2\text{F})^-$ complex would not be feasible in the absence of an automated surface walking algorithm. In arriving at the results presented here, we employed our own surface walking algorithm which is detailed elsewhere.³⁰ This procedure (1) uses local first- and second-derivative data (to move toward or away from local minima), (2) takes "steps" of (variable) length determined by the accuracy of the local quadratic approximation to the actual energy surface, and (3) maps out "stream beds" which connect local minima through transition states. Our Utah MESS-KIT modular electronic structure codes²⁸ generate the CAS-MCSCF analytical energy derivative data used as input for making use of this walking algorithm.

At the geometries determined by the MCSCF calculations for the $\text{H}^- + \text{HF}$ and $\text{H}_2 + \text{F}^-$ asymptotes as well as at the geometries of the stationary points (where the gradients vanish), full

fourth-order many-body perturbation theory³¹ was used to calculate energies that include a higher level of correlation. In addition to these single-geometry MBPT(4) calculations, coupled-cluster methods were used to obtain even more accurate geometries for the $\text{H}^- + \text{HF}$ and $\text{H}_2 + \text{F}^-$ asymptotes and the HHF⁻ complex. The coupled-cluster model used for these calculations includes all single and double excitations.³² Triple excitations are included in a single noniterative correction referred to as CCSD(T).³³

III. Results and Discussion

As summarized in Table I, we find *no* geometrically stable H-HF complex; as the reaction proceeds energetically downhill along the $\text{H}^- + \text{HF} \rightarrow \text{H}^-\text{HF}$ path, no point is encountered at which all gradient components vanish and where the Hessian matrix is positive. Instead, an inflection point is found near the geometry $r_{\text{HH}} = 1.193$ Å and $r_{\text{HF}} = 1.068$ Å, at an energy ca. 30 kcal/mol lower than the $\text{H}^- + \text{HF}$ asymptote. This is an unusual and somewhat surprising result; we had expected the "double-well" potential energy profile typical of many A-HB systems. We should mention that when calculations were performed using smaller bases and smaller configuration spaces, a local minimum near $r_{\text{HH}} = 1.44$ Å and $r_{\text{HF}} = 1.00$ Å was found, as was a transition state (lying less than 2 kcal/mol higher in energy) near $r_{\text{HH}} = 1.04$ Å and $r_{\text{HF}} = 1.20$ Å. Both the transition state and the H-HF local minimum disappear as the basis and level of electron correlation are increased.

Moving further along the reaction path stream bed, a linear $(\text{H}_2)\text{F}^-$ complex is located and found at $r_{\text{HH}} = 0.758$ Å and $r_{\text{HF}} = 1.999$ Å at the MCSCF level, and at $r_{\text{HH}} = 0.770$ Å and $r_{\text{HF}} = 1.690$ Å at the CCSD(T) level. This H_2F^- complex lies 33.5 kcal/mol below $\text{H}^- + \text{HF}$. Dissociation of this complex into F^- costs 7.0 kcal/mol on the electronic energy hypersurface; thus, the $\text{H}^- + \text{HF} \rightarrow \text{H}_2 + \text{F}^-$ reaction is predicted to be electronically exoergic by 26.5 kcal/mol. The harmonic vibrational frequencies of the linear H_2F^- complex are predicted to consist of a "soft" intermolecular $\text{H}_2\cdots\text{F}^-$ stretch (292 cm^{-1}), a stiffer bending motion (773 cm^{-1}), and an H-H stretching vibration (4143 cm^{-1}). A sense of the accuracy of these frequencies can be gained by comparing our HF (4284 and 4087 cm^{-1}) and H_2 (4224 and 4378 cm^{-1})

(31) (a) Bartlett, R. J. *Annu. Rev. Phys. Chem.* **1981**, *32*, 359. (b) Bartlett, R. J.; Silver, D. M. *Chem. Phys. Lett.* **1974**, *29*, 199. (c) Bartlett, R. J.; Silver, D. M. *Chem. Phys. Lett.* **1977**, *50*, 190.

(32) (a) Purvis, III, G. D.; Bartlett, R. J. *J. Chem. Phys.* **1982**, *76*, 1910. (b) Bartlett, R. J.; Purvis, III, G. D. *Phys. Scr.* **1980**, *21*, 255.

(33) (a) Raghavachari, K.; Trucks, G. W.; Pople, J. A.; Head-Gordon, M. *Chem. Phys. Lett.* **1989**, *157*, 479. (b) Bartlett, R. J.; Watts, J. D.; Kucharski, S. A.; Noga, J. *Chem. Phys. Lett.* **1990**, *165*, 513.

(30) Nichols, J. A.; Taylor, H.; Schmidt, P. P.; Simons, J. *J. Chem. Phys.* **1990**, *92*, 340.

frequencies to those reported by Herzberg³⁴ (4139 and 4395 cm⁻¹, respectively).

Recent experimental findings³⁵ of the Neumark group raise the possibility that photodetachment may produce H₂F in more than one electronic state. At the equilibrium geometry of the (H₂F)⁻ complex we computed the vertical electron detachment energies to produce the ²Σ and ²Π states of H₂F neutral. At the CCSD(T) level of theory, we find that the vertical detachment energy to the ²Σ neutral is 83.8 kcal/mol (3.63 eV). The ²Π state of the neutral is 5.8 kcal/mol (0.25 eV) above the ²Σ state.

These primary findings can be summarized as follows: (i) The H-HF complex does not exist. (ii) The H₂F⁻ complex is linear

(34) *Molecular Spectra and Molecular Structure*; Herzberg, G., Ed.; Van Nostrand: New York, 1950; Vol. I.

(35) Weaver, A.; Metz, R. B.; Bradforth, S. E.; Neumark, D. M. *J. Chem. Phys.*, submitted for publication.

and lies 31.3 kcal/mol below H⁻ + HF when zero-point corrections are considered. (Recall that basis set superposition errors amount to no more than 1 kcal/mol.) This complex has the vibrational frequencies and the geometry detailed in Table I. (iii) The H₂F⁻ complex is stable with respect to H₂ + F⁻ by 4.7 kcal/mol when zero-point corrections are included. (iv) The reaction exothermicity for H⁻ + HF → H₂ + F⁻ is predicted to be -26.6 kcal/mol, including zero-point energies. The latter result is comparable to that computed by using tabulated energies of formation (-30 kcal/mol).

Acknowledgment. We thank J. D. Watts and R. J. Bartlett of the Quantum Theory Project, University of Florida, for making the computer code necessary for evaluating the noniterative CCSD(T) triples corrections available to us. We acknowledge the financial support of the National Science Foundation (Grant CHE-8814765).

Near-UV Absorption Cross Sections and Trans/Cis Equilibrium of Nitrous Acid

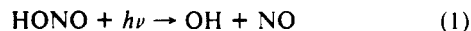
A. Bongartz, J. Kames, F. Welter, and U. Schurath*

Institut für Physikalische Chemie der Universität Bonn, D-5300 Bonn 1, FRG (Received: July 11, 1990)

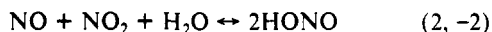
The A ¹A'' ← X ¹A' absorption spectrum of gaseous nitrous acid has been measured in the 300–400-nm range. Absolute cross sections were determined by a combination of gas-phase and wet chemical analysis. The cross sections of prominent bands are 25% larger than the recommended values of Stockwell and Calvert. The influence of spectral resolution on absolute and differential absorption cross sections was also investigated. The integrated band area of the nπ* transition yields an oscillator strength $f = (8.90 \pm 0.36) \times 10^{-4}$, less than the reported liquid phase value of 2×10^{-3} . The equilibrium constant $K = p_{\text{trans}}/p_{\text{cis}}$, based on the assumption that the oscillator strength of the nπ* transition is the same for both rotamers, was found to be 3.25 ± 0.30 at 277 K. This yields an energy difference ΔE between *trans*- and *cis*-HONO of -2700 J mol⁻¹ in the electronic ground state, and -6000 J mol⁻¹ in the excited state.

1. Introduction

Although sources and typical ambient mixing ratios of gaseous nitrous acid in the atmosphere were unknown at the time, the photolysis of HONO¹



held a key position in early photochemical smog models,^{2,3} because it provided a rationale for the presence of OH radicals in polluted atmospheres. Later on, when the UV photolysis of ozone and the subsequent reaction O(¹D) + H₂O → 2OH was included in the kinetic schemes,^{4,5} the general importance of HONO as a source of OH radicals was called in question. Reaction 2,⁶ and other



HONO-producing reactions of the NO_x-H₂O system,⁷ were found to be surface-catalyzed and too slow in the homogeneous gas phase to constitute significant sources of HONO under atmospheric conditions. Indirect evidence of unreasonably high HONO

concentrations in polluted air was first obtained by a wet chemical technique.⁸ This method, as well as more recent denuder techniques,⁹ suffers severe interferences by other nitrogen compounds. Nighttime mixing ratios of up to 8 ppb HONO in very polluted air were unambiguously identified by long path differential optical absorption spectroscopy (DOAS) in the near-UV region,^{10,11} where HONO exhibits a characteristic banded absorption spectrum.¹² In cleaner air masses the mixing ratio always dropped below the detection limit of less than 100 ppt. As pointed out in a recent review article,¹³ the sensitivity of DOAS with respect to HONO is superior to most other analytical techniques.

Quantitative determination of HONO by DOAS requires absolute absorption cross sections and a well-resolved UV spectrum. However, such data are unavailable by standard laboratory techniques, because the gaseous compound can only be generated in the presence of other UV-absorbing species,^{1,12} and the published absorption cross sections of HONO¹⁴⁻¹⁶ differ by as much as a factor of 4. The most recent absorption cross sections, which are recommended by the NASA Panel for Data Evaluation,¹⁷ were

(1) Cox, R. A. *J. Photochem.* **1974**, *3*, 175-188.

(2) Eschenroeder, A. Q.; Martinez, J. R. *Adv. Chem. Ser.* **1972**, *113*, 101-168.

(3) Kerr, J. A.; Calvert, J. G.; Demerjian, K. L. *Chem. Br.* **1972**, 252-257.

(4) Levy, H. H. *Science* **1971**, *173*, 141-143; *Planet. Space Sci.* **1972**, *20*, 919-935.

(5) Weinstock, B. *Science* **1969**, *166*, 224-225.

(6) Kaiser, E. W.; Wu, C. H. *J. Phys. Chem.* **1977**, *81*, 1701-1706.

(7) Sakamaki, F.; Hatakeyama, S.; Akimoto, H. *Int. J. Chem. Kinet.* **1983**, *15*, 1013-1029.

(8) Nash, T. *Tellus* **1974**, *26*, 175-179.

(9) Ferm, M.; Sjödin, A. *Atmos. Environ.* **1985**, *19*, 979-983.

(10) Perner, D.; Platt, U. *Geophys. Res. Lett.* **1979**, *16*, 917-920.

(11) Harris, G. W.; Carter, P. L.; Winer, A. M.; Pitts, J. N.; Platt, U.; Perner, D. *Environ. Sci. Technol.* **1982**, *16*, 414-419.

(12) King, G. W.; Moule, D. *Can. J. Chem.* **1962**, *40*, 2057-2065.

(13) Platt, U. In *Chemistry of Multiphase Atmospheric Systems*; Jaeschke, W., Ed.; Springer: Berlin, 1986; pp 299-319.

(14) Johnston, H. S.; Graham, R. *Can. J. Chem.* **1974**, *52*, 1415-1423.

(15) Cox, R. A.; Derwent, R. G. *J. Photochem.* **1976/77**, *6*, 23-34.

(16) Stockwell, W. R.; Calvert, J. G. *J. Photochem.* **1978**, *8*, 193-203.